JOURNAL OF BACTERIOLOGY, Dec. 1997, p. 7394–7402 Vol. 179, No. 23
0021-9193/97/$04.00+0

Interaction of *Bacillus subtilis* Purine Repressor with DNA†

BYUNG SIK SHIN,[1] ARNOLD STEIN,[2] AND HOWARD ZALKIN[1]*

Departments of Biochemistry[1] and Biological Sciences,[2] Purdue University, West Lafayette, Indiana 47907

Received 17 July 1997/Accepted 23 September 1997

A purine repressor (PurR) mediates adenine nucleotide-dependent regulation of transcription initiation of the *Bacillus subtilis pur* operon. This repressor has been purified for the first time, and binding to control site DNA was characterized. PurR binds in vitro to four operons. Apparent K_d values for binding were 7 nM for the *pur* operon, 8 nM for *purA*, 13 nM for *purR*, and 44 nM for the *pyr* operon. In each case, DNase I footprints exhibited a pattern of protected and hypersensitive sites that extended over more than 60 bp. A GAAC-N_{24}-GTTC sequence in the *pur* operon was necessary but not sufficient for the PurR-DNA interaction. However, this motif, which is conserved in the four binding sites, was not required for binding of PurR to *purA*. Thus, the common DNA recognition element for binding of PurR to the four operons is not known. Multiple PurR-*pur* operon DNA complexes having a binding stoichiometry that was either approximately two or six repressor molecules per DNA fragment were detected. The results of a torsional constraint experiment suggest that control site DNA forms one right-handed turn around PurR.

The genes required for de novo synthesis of IMP are clustered in a 12-gene polycistronic operon in *Bacillus subtilis* (10). Transcription of the *pur* operon is subject to dual regulation. The addition of adenine to cells results in the repression of transcription initiation, whereas the addition of guanine signals premature transcription termination in the 242-nucleotide (nt) mRNA leader region preceding the first gene of the operon. A purine repressor (PurR) is required for the regulation of transcription initiation (11). The repressor is a 62-kDa homodimer containing 285 amino acid subunits (31) encoded by a *purR* gene at about 6° in a sequenced region (19) of the *B. subtilis* chromosome. The *pur* operon DNA site to which the crude repressor bound was mapped to a position corresponding to approximately −136 to −26 relative to the start of transcription (11). This site is contiguous with and overlaps the −35 promoter element at nts −33 to −28. Binding of PurR to the *pur* operon control site was blocked by phosphoribosylpyrophosphate (PRPP) leading to a model in which the excess adenine signal is transmitted to PurR by the PRPP pool (31). It was proposed that upon uptake, adenine is converted to adenine 5′ nucleotides and that the resulting allosteric inhibition of PRPP synthetase by ADP (1) lowers the PRPP pool levels (26), permitting PurR to bind to and repress the transcription of the *pur* operon. *B. subtilis* PurR bears no amino acid sequence similarity to *Escherichia coli* PurR. Furthermore, there is no similarity in the DNA control sites for these two repressors or in the purine or purine nucleotide signals that modulate binding to the DNA control sites.

There is presently no information about what determines *B. subtilis* PurR-*pur* operon DNA binding specificity. It has been noted, however, that PurR also binds to *purR* and to *purA* (31), but the common recognition determinant is unknown. The *purA* gene encodes the first enzyme in the two-step branch from IMP to AMP. This gene is not part of the *pur* operon and, as a result, *purA* expression is not repressed by guanine. In this report, we describe the purification of PurR and the first studies of the PurR-DNA interaction using purified repressor. We compare the binding of the purified repressor to 5′-flanking DNA in four genes or operons: the *pur* operon, *purA*, *purR*, and the *pyr* operon. A common recognition determinant has not been identified. Upon binding of a PurR minicircle, one positive supercoil is introduced into the DNA control site, supporting a model in which control site DNA wraps around the repressor.

MATERIALS AND METHODS

Bacterial strains and plasmids. *E. coli* DH5α was used for plasmid constructions, and strain B834(DE3) (9) was used for *purR* overexpression. Plasmid pMW10 (31) is a *purR*$^+$ derivative of pT7-7 in which expression is controlled by a phage T7 promoter. Plasmid pR6H is a pMW10 derivative in which six histidine codons are fused onto the 3′ end of *purR*. Other plasmids containing segments of 5′-flanking control site DNA from the indicated operons ligated into the pUC19 or pUC118 polylinker are listed in Table 1.

Construction of plasmids. Six histidine codons were attached to the 3′ end of *purR* by PCR with oligonucleotides Pur5 and Pur6 (Table 1) and with pMW10 as the template DNA. The PCR product of 575 bp was digested with *Eco*RV and *Hin*dIII and was used to replace the corresponding fragment of pMW10, thus generating pR6H. Plasmids pUC118-*pur127*, pUC118-*pur186*, pUC19-*pur196*, pUC118-*purA*, pUC118-*purR*, and pUC118-*pyr*, containing the 5′-flanking control sites for the *pur* operon, *purA*, *purR*, and the *pyr* operon, were constructed by ligating into a cloning vector the respective DNA control site prepared by PCR with the primers shown in Table 1.

PurR purification. *E. coli* B834(DE3) transformed with plasmid pR6H was grown in 5 liters of Luria-Bertani medium containing 50 μg of ampicillin per ml to the mid-exponential phase. The addition of 1% lactose was then used to induce T7 RNA polymerase, and growth was continued for 16 h at 30°C. Cells were harvested by centrifugation and resuspended in 80 ml of buffer A (50 mM sodium phosphate [pH 8.0], 300 mM NaCl) containing 1% phenylmethylsulfonyl fluoride. All purification steps were performed at room temperature. After incubation with 10 mg of DNase I and 0.5 mg of RNase H for 30 min, cells were disrupted by two passes through a French press at 12,000 lb/in^2. The resulting extract was clarified by centrifugation at 20,000 × *g* for 30 min, and 40 ml of a 50% suspension of Ni^{2+}-nitrilotriacetic acid–agarose (Ni-NTA resin; QIAGEN) equilibrated in buffer A was added to the supernatant. The suspension was stirred gently for 2 h and then poured into a 1.5-cm-diameter column. The column was washed sequentially with 400 ml of buffer A and 400 ml of buffer B (50 mM sodium phosphate [pH 6.0], 300 mM NaCl, 10% glycerol). Bound PurR was eluted with a 300-ml gradient of 0 to 0.3 M imidazole in buffer B. Fractions were analyzed by electrophoresis on sodium dodecyl sulfate (SDS)–12% polyacrylamide gels. Fractions of the essentially pure protein were combined and dialyzed against 10 mM HEPES (pH 8.0)–50 mM ammonium sulfate–300 mM NaCl. After concentration by ultrafiltration to approximately 10 mg/ml, the protein was frozen at −80°C in 50-μl aliquots.

Protein-DNA binding. Gel retardation assays were carried out as described previously (11). A typical assay mixture contained 10 mM HEPES (pH 7.6), 50 mM KCl, 10% glycerol, 1 mM EDTA, 5 mM $MgCl_2$, 5 mM dithiothreitol, 5 μg of double-stranded poly(dI-dC) per ml, approximately 10 fmol of ^{32}P-end-la-

* Corresponding author. Phone: (765) 494-1618. Fax: (765) 494-7897.

† Journal paper 5546 from the Purdue University Agricultural Research Station.

TABLE 1. Plasmids and oligonucleotides used in this study[a]

Plasmid and primer	Sequence (5′→3′)	Gene	nt[b]
pR6H			
Pur5	5′-TTAACGGATATCTTAGGAAAGG (*Eco*RV)[c]	*purR*	316[d]
Pur6	5′-CCCAAGCTTCTATTAGTGATGATGATGATGTGATTCTGTCTCTCCATTCTTT (*Hin*dIII)	*purR*	—[e]
pUC118-*pur127*			
675	5′-GCGTGAATTCGGATAATGTCAACGAT (*Eco*RI)	*pur*	−21
676	5′-GTCAGGATCCAGGAAAATGGGTCAATTCAG (*Bam*HI)	*pur*	−147
pUC118-*pur186*			
163	5′-GATATCTGCCTGTAAGTCGACTGG (*Sal*I)	*pur*	−183
164	5′-GAGGTCGTGTTTTGTCGACATGTT (*Sal*I)	*pur*	+3
pUC19-*pur196*			
474	6′-GACCAAGCTTGATATCTGCCTGTAAGGCGA (*Hin*dIII)	*pur*	−193
459	5′-GTCGTGTTTTGAATTCATG (*Eco*RI)	*pur*	+3
pUC118-*purA*			
268	5′-CAGGCAAGGATCCTTTCTTATGC (*Bam*HI)	*purA*	−163
269	5′-CAACTACTGAATTCATGTCGG (*Eco*RI)	*purA*	+47
pUC118-*purR*			
407	5′-GCGACGAGAATTCATGAAC (*Eco*RI)	*purR*	+2[d]
408	5′-GTGCTTGGATCCGTTACAC (*Bam*HI)	*purR*	−268[d]
pUC118-*pyr*			
467	5′-GGTTTTGAGGATCCACGAAC (*Bam*HI)	*pyr*	−133
468	5′-CAGCTTTTGAATTCAATGTGTG (*Eco*RI)	*pyr*	+166

[a] Primers were used for amplification of gene fragments inserted into pUC19 or pUC118 to yield the indicated plasmid.
[b] Positions relative to the transcription start site after the PCR product was digested with the indicated restriction enzymes, unless otherwise indicated.
[c] Restriction sites are underlined.
[d] Relative to the translation start site.
[e] —, six His codons were added to *purR* at the 3′ end.

beled DNA probe (approximately 2,000 cpm), and PurR protein in a volume of 20 μl. Unless noted otherwise, a *pur* operon DNA fragment from nts −147 to −21 was used. After incubation for 20 min at room temperature, 10 μl of the mixture was loaded immediately onto a 4% polyacrylamide gel in 90 mM Tris-borate (pH 8.3)–2 mM EDTA and electrophoresed at 10 V/cm for 2 h. Dried gels were visualized by autoradiography and quantitated with a Packard Instant Imager. Apparent K_d values were calculated from isotherms of free DNA at various repressor concentrations according to the Hill equation with Ultrafit software (Biosoft, Cambridge, United Kingdom). Apparent K_d values are not true dissociation constants because of the formation of multiple repressor-DNA complexes (see Fig. 2). The repressor concentration was calculated on the basis of the 31-kDa subunit.

DNase I footprinting was carried out with ^{32}P-end-labeled DNA fragments incubated with PurR as described for gel retardation. For DNase I digestion, 50 μl of 5 mM $CaCl_2$ was added to the 50-μl protein-DNA mixture, followed by 0.17 U of DNase I. Digestion was stopped after 1 min at room temperature by the addition of 100 μl of a stop solution (200 mM NaCl, 30 mM EDTA, 1% SDS, 10 μg of yeast tRNA). Samples were extracted with phenol-chloroform-isoamyl alcohol (25:24:1, vol/vol/vol), precipitated with ethanol at −80°C for 20 min, and centrifuged. Precipitated DNA was washed with 70% ethanol, dried, taken up in formamide sequencing gel buffer, and electrophoresed on an 8% polyacrylamide sequencing gel alongside a Maxam-Gilbert A+G sequencing ladder (24) for the same fragment.

Methylation interference was carried out as described previously (2). The 5′ end of either the top or the bottom strand of a *pur* operon DNA fragment from nts −193 to +3 was labeled with [γ-^{32}P]ATP. After methylation, 10 μg of tRNA carrier was added, and the DNA was precipitated twice and washed with ethanol. Binding of PurR to methylated DNA was carried out as described above for the gel retardation assays with reaction mixtures that were scaled up 10-fold. After electrophoresis on a 5% nondenaturing gel, free and bound DNAs were isolated, subjected to piperidine cleavage, and analyzed on 8% denaturing sequencing gels.

Construction of minicircles. A 628-bp *Hae*II fragment from plasmid pUC118-*pur186* containing the *pur* operon control region (nts −183 to +3) was dephosphorylated with alkaline phosphatase, purified, and labeled with [γ-^{32}P]ATP by use of T4 polynucleotide kinase. Circularizations were performed by incubating the labeled fragments at a DNA concentration of 0.1 μg/ml in 10 mM Tris-HCl (pH 7.5)–50 mM NaCl–10 mM $MgCl_2$–5 mM dithiothreitol–0.25 mM ATP–0.1 mg of bovine serum albumin per ml with 1.0 U of T4 DNA ligase per ml for 3 h at room temperature. Ethidium bromide was added to the ligation reaction mixture at a concentration of 0, 0.15, or 0.3 μg/ml to obtain three samples with different numbers of supercoils (35). After ligation, each sample was adjusted to 1% (wt/vol) SDS–1 M NaCl and extracted with 1 volume of chloroform-isoamyl alcohol (24:1, vol/vol), and the DNA was precipitated with ethanol. Samples were applied to a 4% polyacrylamide gel to identify the topoisomers (35).

Torsional constraint assay. Topoisomerase relaxations were carried out as described previously (17). Approximately 25 fmol of each labeled topoisomer was incubated in the presence or absence of 10 ng of PurR in 20 μl of DNA binding buffer as described for gel retardation assays. The resulting PurR-DNA complexes were treated with 10 U of topoisomerase I (Bethesda Research Laboratories, Inc.), and the incubation was continued for 4 h at room temperature. The reaction mixture was extracted with phenol-chloroform-isoamyl alcohol (25:24:1, vol/vol/vol). DNA was precipitated with ethanol and electrophoresed on a 4% acrylamide gel in the presence of 0.3 μg of ethidium bromide per ml as described by Zivanovic et al. (35). The gel was prerun for 2 h at a voltage gradient of 10 V/cm at room temperature and, after samples were applied, electrophoresis was carried out at the same voltage until the xylene cyanol blue dye reached almost the bottom of the gel. In the presence of 0.3 μg of ethidium bromide per ml, the nicked circles were separated from the topoisomers.

PurR-DNA binding stoichiometry. To prepare ^{35}S-labeled PurR, *E. coli* B834(DE3) cells containing pR6H were grown overnight at 37°C in 2 ml of NMM (3) containing 0.8 mM methionine but without supplementation with the other 19 amino acids. A 1-ml aliquot was used to inoculate 100 ml of the same medium. Growth was continued for 6 h to an optical density at 600 nm of ~0.5. Lactose at a final concentration of 1% was added to induce T7 RNA polymerase for overexpression of *purR*. At the same time, 1 mCi of [^{35}S]methionine (1,175 Ci/mmol) was added, and growth was continued for 12 h. ^{35}S-labeled PurR was purified by Ni-NTA–agarose chromatography as described for the unlabeled protein.

PurR-DNA binding reaction mixtures contained 2 pmol of ^{32}P-end-labeled DNA (~8,000 cpm) and 3 to 16 pmol of ^{35}S-PurR (~300 to 1,600 cpm). DNA bands were localized by autoradiography and excised from the gel. Other parts of the gel were excised to determine background radioactivity. Samples of ^{35}S-PurR and [^{32}P]DNA were added to control gel slices to determine specific radioactivity under the same conditions. Slices were digested with a mixture of 21% H_2O_2 and 17% $HClO_4$ overnight at 60°C in glass scintillation vials. After the

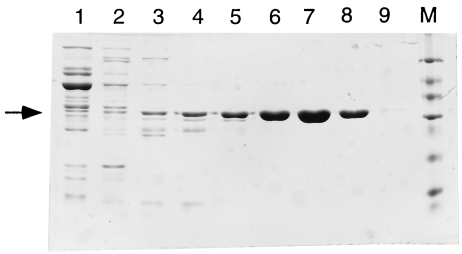

FIG. 1. Purification of PurR. SDS-polyacrylamide gel electrophoresis results are shown for a soluble cell extract (lane 1), flowthrough from an Ni-NTA–agarose column (lane 2), and fractions eluted by the imidazole gradient (lanes 3 to 9). Fractions corresponding to lanes 6 to 8 were pooled. The arrow shows PurR. Molecular mass standards (lane M) in kilodaltons are, from top to bottom, 66, 45, 36, 29, 24, 20, and 14.

vials were cooled, 14 ml of scintillation solution (EcoLume; ICN Pharmaceuticals) was added, and the vials were dark adapted for 1 day. Radioactivity was counted in a Beckman LS 1801 instrument with two windows. Window 1 (0 to 700) contained 100% of the ^{35}S and 15% of the ^{32}P, whereas window 2 (700 to 950) contained 85% of the ^{32}P. Corrections were made for the spillover radioactivity. Sample radioactivity was counted to a 95% confidence level of 2.0 sigma. Background radioactivity was counted in a slice from an unused portion of the gel.

RESULTS

PurR purification. PurR was overproduced in *E. coli* B834 (DE3) and purified in a single step by Ni-chelate affinity chromatography as described in Materials and Methods. Although PurR was an abundant protein in cells following overexpression, a substantial fraction was insoluble. Consequently, PurR comprised only a small percentage of the proteins in the soluble cell extract (Fig. 1, lane 1). Extract proteins were adsorbed to Ni-NTA–agarose, and the repressor was eluted by approximately 0.2 M imidazole. Fractions corresponding to lanes 6 to 8 in Fig. 1 were pooled to yield a preparation exceeding 95% homogeneity. The yield was approximately 100 mg of purified protein from 5 liters of *E. coli* cells. DNA binding activity tested with a standard assay (see Materials and Methods) and inhibition of DNA binding by PRPP (31) were similar for native PurR and PurR having the CO_2H-terminal His tag (data not shown). Cell extracts were used for these experiments because the native protein was refractory to purification.

Binding of PurR to DNA. Weng et al. (31) reported that crude PurR bound to the 5′-flanking regions of three mono- or polycistronic operons: the *pur* operon, *purR*, and *purA*. In addition, PurR was found to bind to the 5′-flanking region of the *pyr* operon. In earlier experiments with crude extracts, quantitation of binding affinity was not possible. We have determined apparent dissociation constants for binding of the purified repressor to the promoter regions of these genes using a gel retardation assay. The DNA fragments used for PurR binding are identified in Table 1. These DNA fragments overlap or are contiguous with the promoter in the case of the *pur* operon, *purA*, and the *pyr* operon. Since the *purR* promoter has not been mapped, the *purR* DNA used to probe repressor binding covers the region from nts −268 to +2 relative to the start of translation. The results of gel retardation are shown in Fig. 2. PurR binding was complicated by the formation of multiple complexes with DNA. This result is seen most clearly for the gel shifts with *pur* operon, *purA*, and *purR* DNAs. Binding isotherms were therefore calculated from the decrease in the levels of unbound DNA, and apparent K_d values represented the PurR concentration required for 50% saturation of the control site DNA. The apparent K_d values determined from these data were as follows: *pur* operon, 7.0 ± 1.0 nM; *purA*, 7.9 ± 0.8 nM; *purR*, 12 ± 0.8 nM, and *pyr* operon, 43 ± 22 nM. Binding specificity was shown by a competition experiment. A 300-fold excess of pUC18 DNA cut by *Sau*3A produced no detectable inhibition of PurR-*pur* operon binding (data not shown).

DNase I footprinting was used to identify and compare the PurR binding sites in the four genes. The same DNA fragments that were used for the measurement of PurR binding affinity (shown in Fig. 2) were used for the DNase I footprinting experiments shown in Fig. 3. For each footprint, there is an extended region that is protected from DNase I digestion and that is interspersed with sites hypersensitive to DNase I cleavage. These patterns of protection and hypersensitivity are shown schematically in Fig. 4. The DNase I footprint of the *pur* operon, shown in Fig. 3 and 4, covered over 90 bp, extending from nt −122 to the −30 promoter site. Although not shown in Fig. 3 and 4, footprinting experiments with a longer DNA fragment (−193 to +3) indicated that the 5′ boundary extends to position −163 on the top strand and −179 on the bottom strand. Protected and hypersensitive positions in the upstream segment from −179 to −122 were less well defined than those shown in Fig. 3 and summarized in Fig. 4. The *pur* operon footprint shown in Fig. 4 is similar to that found earlier with a crude PurR fraction (11). The patterns of protection and hypersensitivity for *purA* match those for the *pur* operon and occur in similar positions relative to the site for transcription initiation. A less well defined pattern of protected and hypersensitive sites extends to *purA* nt −136 (data not shown). The *purA* and *pur* operon control sites to which PurR binds share a 20-bp protected core region flanked by protected and hypersensitive sites having approximately 10-bp periodicity. Otherwise, there is little significant sequence similarity between these PurR sites in *purA* and the *pur* operon. Each site does, however, have a 5′-GAAC-N-GTTC dyad symmetry in which the upstream GAAC sequence is in the 20-bp protected core region. The numbers of intervening nucleotides, N, in this motif are 24 in the *pur* operon and 25 in *purA*. Footprint patterns for the *pyr* operon and *purR*, shown in Fig. 4, are dissimilar to those for the *pur* operon and *purA*. However, both footprints cover 60 to 80 bp, have alternating protected and hypersensitive sites, and have sequences related to the GAAC-N-GTTC dyad symmetry in the *pur* operon and *purA*. The repressor binding site in the *pyr* operon is contiguous with the promoter, as in the control sites in *purA* and the *pur* operon.

To characterize further the *pur* operon control site, methylation interference was carried out to identify purine residues that contact the protein. After methylation of the *pur* operon control region in a −193 to +3 DNA fragment, fractions of PurR-bound and unbound DNAs were isolated from a gel shift assay, subjected to piperidine cleavage, and run on a polyacrylamide sequencing gel. For this analysis, it was necessary to carry out the PurR-DNA gel shift assay at a protein concentration that resulted in approximately 50% binding to methylated DNA. At higher protein concentrations, the methylated DNA was fully bound by PurR, indicating that single methylations had only a small effect on PurR binding affinity. Figure 5 shows the methylation interference pattern of the *pur* operon control site. PurR binding affinity was decreased by methylation of G residues at positions −75 and −47 on the top strand and G residues at positions −72 and −44 on the bottom strand. This pattern corresponds to guanine methylation in the GAAC-N_{24}-GTTC motif.

A series of mutations was constructed and analyzed to determine the importance of the GAAC-N_{24}-GTTC dyad symmetry for PurR binding. Replacements were made in various

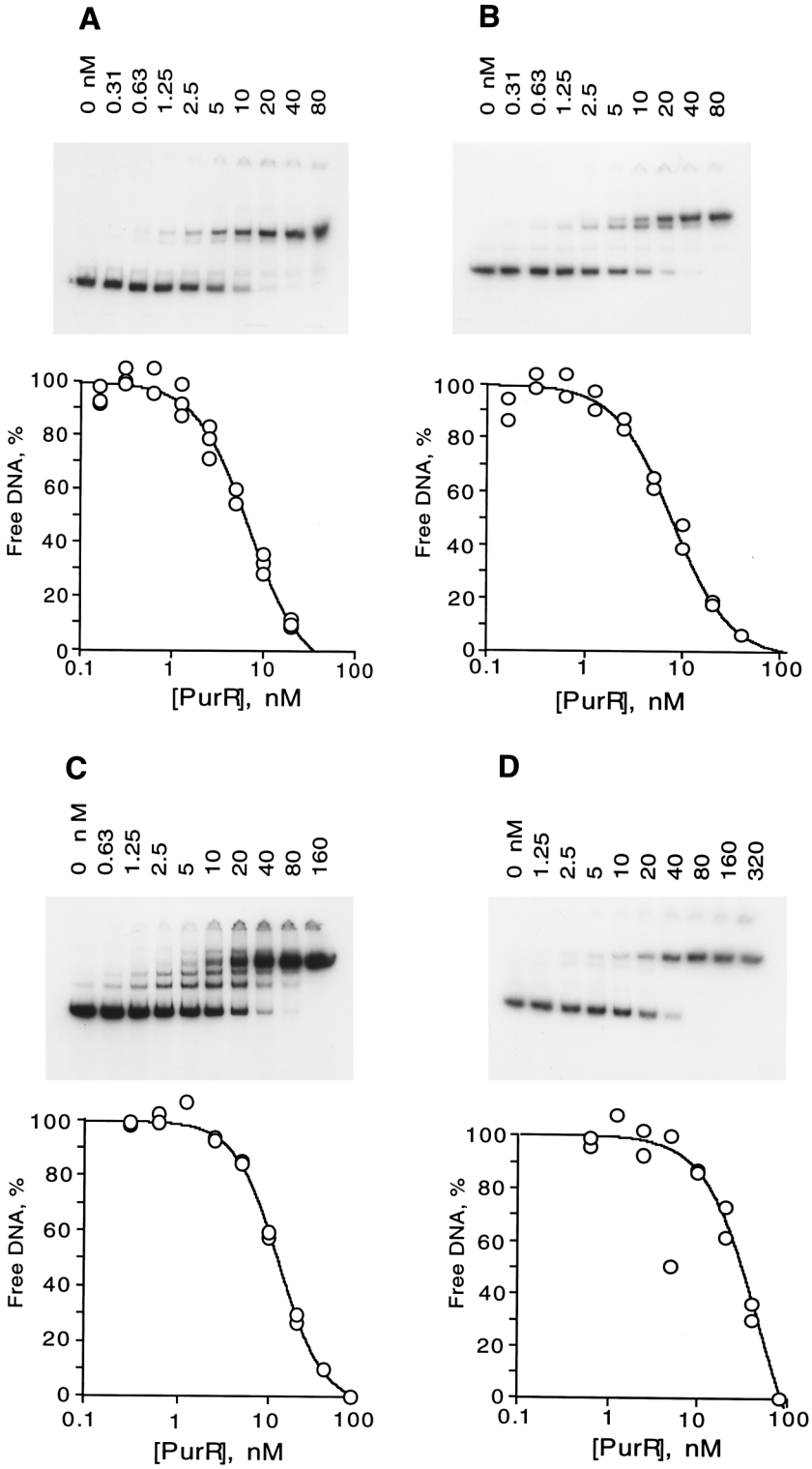

FIG. 2. Binding of PurR to control region DNA. Profiles of gel retardation binding assays are shown along with the calculated binding isotherms for the *pur* operon with pUC118-*pur127* (A); *purA* with pUC118-*purA* (B); *purR* with pUC118-*purR* (C); and the *pyr* operon with pUC118-*pyr* (D). Binding isotherms include data combined from two experiments. PurR concentrations are given at the top of each gel.

positions of each half of the motif. The data in Fig. 6 show that replacement of the GAAC sequence at positions −75 to −72 in *pur-10* increased the apparent K_d by more than 10-fold, whereas replacement of the downstream GTTC sequence (*pur-20*) had little, if any, effect on PurR binding. PurR binding affinity was decreased in the *pur-30* double mutant, but quantitation was difficult as a result of weak binding. Decreased PurR binding affinity in the *pur-12* and *pur-13* mutants sug-

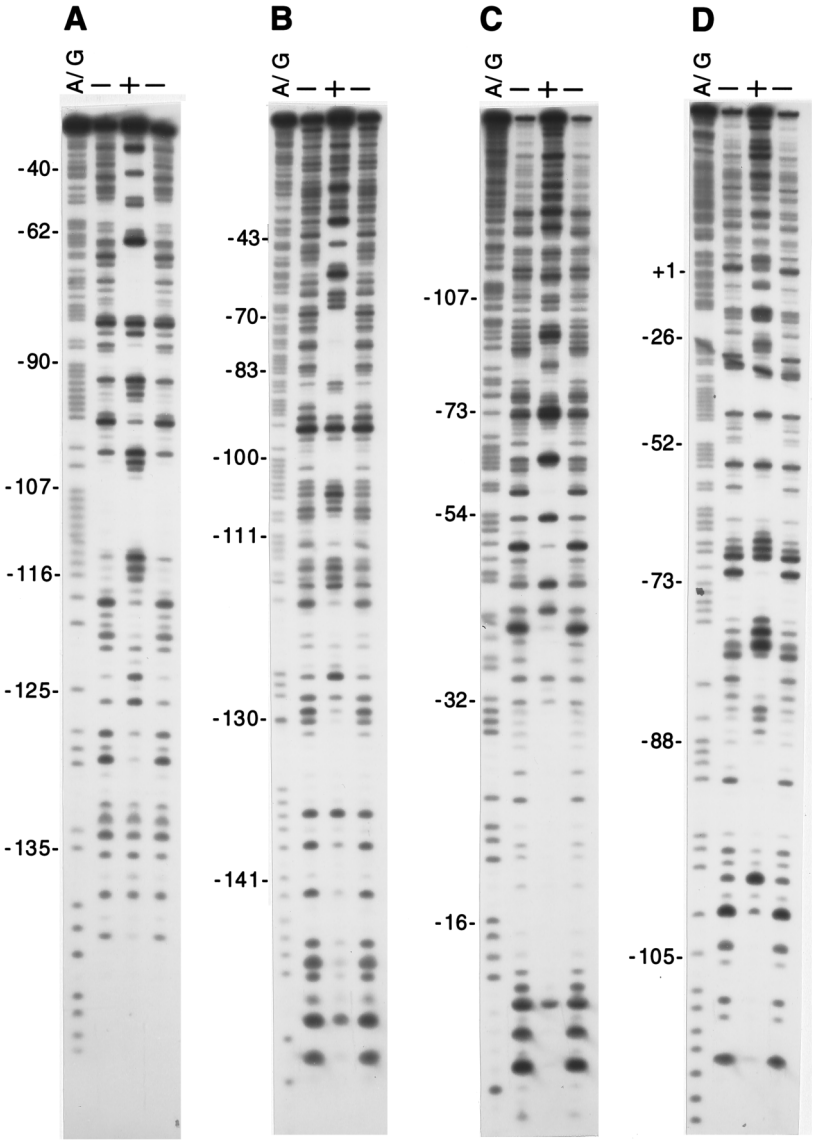

FIG. 3. DNase I footprints of PurR binding sites. (A) *pur* operon. (B) *purA*. (C) *purR*. (D) *pyr* operon. The 5′ end of the top strand was labeled for *pur*, *purA*, and *pyr* DNAs. The 5′ end of the bottom strand was labeled for *purR* DNA. In each set, the gel lanes, from left to right, contain an A+G sequencing ladder, no PurR, PurR, and no PurR. Positions relative to the start of transcription are given for the *pur* operon, *purA*, and the *pyr* operon. For *purR*, positions are relative to the start of translation.

gested that each of the G residues has a role in binding. Although the GAAC-N_{24}-GTTC motif is important for PurR binding, it is not sufficient. PurR at a concentration of 640 nM was not bound to a 36-bp fragment, (nts −77 to −42, containing the motif), indicative of a >100-fold-decreased binding affinity compared with that for the intact site.

Binding stoichiometry. Multiple repressor-DNA complexes were formed in gel shift assays with *pur* operon, *purA*, and *purR* control site DNA fragments (Fig. 2) (see also references 9 and 28). The number of PurR-*pur* operon DNA complexes depended on the fragment length. Two well-separated PurR-DNA complexes were obtained with a 127-bp fragment, and three were detected with a 196-bp fragment (Fig. 7 and Table 2). We determined the PurR binding stoichiometry for *pur* operon DNA with direct counts for ^{35}S-labeled protein and ^{32}P-labeled DNA (Fig. 7 and Table 2). Binding to complexes B1 and B2 was approximately two PurR dimers per DNA fragment. The basis for the electrophoretic mobility difference between B1 and B2 is not known. In complex B3, the binding stoichiometry was approximately six PurR dimers per 196-bp DNA fragment.

Effect of PurR binding on the topology of the DNA control site. Similarities between DNase I footprints of *E. coli* DNA gyrase binding sites and the *B. subtilis pur* operon control region have been noted (11) and have led to the suggestion that DNA may wrap around PurR. We used the torsional constraint assay (13) to assess the topology of DNA bound to PurR. A 628-bp minicircle carrying the −183 to +3 *pur* operon control site was constructed by self-ligation of an *Hae*II fragment isolated from plasmid pUC118-*pur186*. DNA minicircles are highly sensitive to the topological changes induced by topoisomerase I treatment while the DNA is wrapped around a protein (15, 17). Specifically, the linking number change (ΔLk) is measured for the DNA minicircle containing bound protein

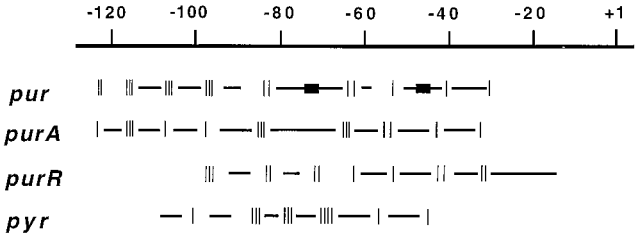

FIG. 4. Summary of the DNase I footprints shown in Fig. 3. Positions of protection from cleavage (short horizontal lines) and hypersensitivity to cleavage (vertical lines) are aligned relative to the start of transcription for the *pur* operon, *purA*, and the *pyr* operon. Positions for *purR* are aligned relative to the start of translation. The location of the GAAC-N_{24}-GTTC motif is shown by black boxes for the *pur* operon.

relative to the protein-free DNA. This topological quantity, which must be an integer, is related to the change in DNA writhing (ΔWr), a measure of its wrapping, through the relationship ΔLk = ΔWr + ΔTw, where ΔTw is the possible change in DNA twist from its ordinary value in B-form DNA (6, 12, 22, 33). Thus, a ΔLk value of −1 would suggest that the DNA is wrapped once around the protein in a left-handed fashion, a ΔLk value of +1 would suggest that the DNA is wrapped once around the protein in a right-handed fashion, and a ΔLk value of 0 would suggest that the DNA does not wrap around the protein at all.

DNA minicircles were prepared in three different topological states as described in Materials and Methods in order to test whether any topological change induced by PurR binding was dependent upon the initial topological state of the minicircle. The three samples that were characterized are shown in Fig. 8A. Under electrophoresis conditions in which there was no ethidium bromide in the gel, the DNA sample that self-ligated in the absence of ethidium bromide (lane 1) possessed predominantly one positive supercoil. This sample also contained nicked and relaxed species that were not resolved. Consistent with this supercoil being positive, the sample ligated in the presence of 0.15 μg of ethidium bromide per ml (lane 2), which must necessarily be less positively supercoiled, lacked the +1 species and was nearly relaxed, running very close to the nicked DNA. The sample ligated in the presence of 0.3 μg of ethidium bromide per ml (lane 3), which must necessarily be more negatively (or less positively) supercoiled than the previous sample, possessed predominantly one negative supercoil that migrated slightly faster than the relaxed DNA. Accordingly, the predominant topoisomers in the three samples are designated +1, 0, and −1, respectively, denoting their supercoiling under these electrophoresis conditions and consistent with the assignments of others (35). Each of the samples also contained nicked DNA that was not resolved from the relaxed minicircles.

The same samples, along with appropriate markers, were also analyzed on a gel that contained 0.3 μg of ethidium bromide per ml (data not shown). The presence of ethidium bromide in the gel at this concentration introduced several positive supercoils into each closed circular DNA molecule. This experiment demonstrated that the three samples each contained predominantly one topoisomer, with ΔLk values differing consecutively from each other by one unit, consistent with the assignment of bands in Fig. 8A. Under these electrophoresis conditions, each of the topoisomers ran as positively supercoiled DNA (data not shown). This result supported the conclusion that the major species in samples 1, 2, and 3 in Fig. 8A are +1, 0, and −1, respectively. However, the exact number of supercoils in each sample is less important here than the fact that this number differs for the three samples.

Figure 8B and C show the results of the torsional constraint assay performed with minicircles that were prepared in the three different topological states (labeled 1, 2, and 3, as in Fig. 8A). This gel, in contrast to that in Fig. 8A, contained 0.3 μg of ethidium bromide per ml. In Fig. 8B, topoisomerase I relaxation was performed in the absence of PurR. As expected for complete relaxation, all three topoisomer mixtures relaxed to the same predominant product, designated ΔLk = 0. The smaller amounts of topoisomers formed at ΔLk = ±1 resulted from thermal fluctuations at the time of DNA closure (8). In Fig. 8C, topoisomerase I relaxation was performed after the DNA minicircles were incubated with PurR. A ΔLk of one unit occurred for all three samples. Thus, ΔLk did not depend upon the initial topological state of the minicircle to which PurR was bound; it depended only upon the nature of the protein-DNA interaction. It is clear that the sign of ΔLk was +1 rather than −1 because all topoisomers on this gel were positively supercoiled and the topoisomers shifted downward from Fig. 8B to Fig. 8C. Under these conditions, faster-migrating topoisomers must be more positively supercoiled and have positive incre-

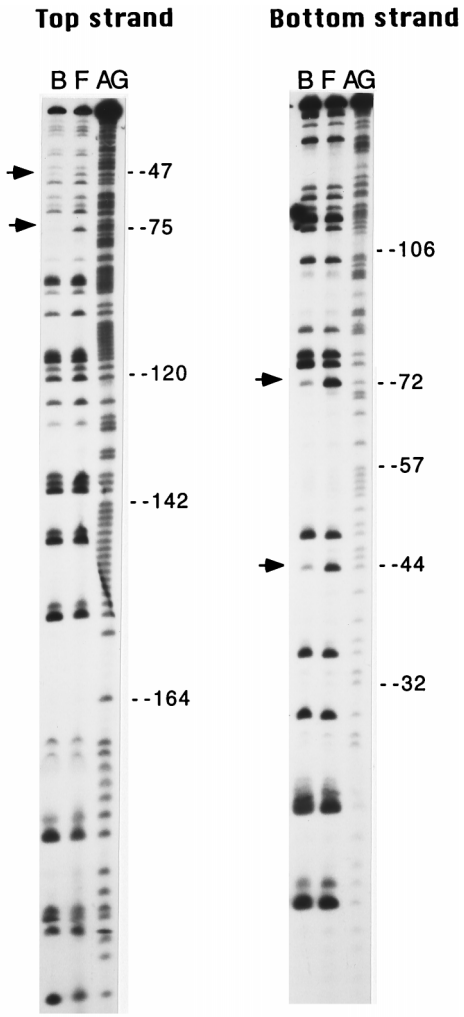

FIG. 5. Effect of guanine methylation on PurR binding. The cleavage pattern after methylation is shown for the top and bottom strands of a −193 to +3 *pur* operon fragment. Lanes: B, DNA bound by PurR; F, free DNA; AG, A+G sequencing ladder. Arrows indicate methylated G residues on each strand.

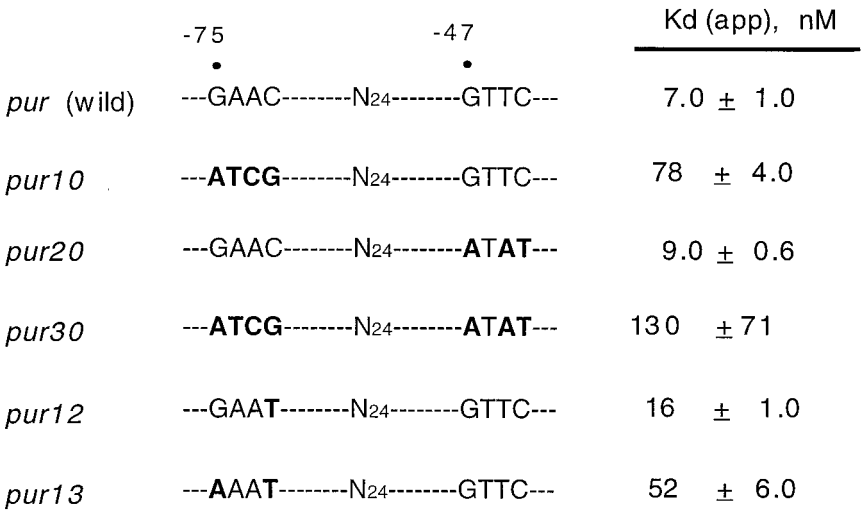

FIG. 6. Diagram showing the effect of mutagenesis on PurR binding to a *pur* operon control site. Apparent (app) K_d values were calculated from binding isotherms similar to those shown in Fig. 2 with DNA fragments (wild type and mutant) from pUC118-*pur127*. Mutations are shown in bold.

ments in ΔLk. This result suggests that DNA wraps once around the bound PurR oligomers in a right-handed fashion.

DISCUSSION

Purines or purine nucleotides are signals for transcriptional regulation of genes in the 14-step de novo biosynthetic pathway leading to the synthesis of AMP and GMP in both *E. coli* and *B. subtilis*. In both organisms, a repressor protein, PurR, binds to a control site that is usually contiguous with or overlaps the promoter and inhibits transcription initiation. However, the structures of the repressors, the sequences of the binding sites, and the type of interaction with DNA, as well as the effectors that modulate binding to DNA, are different. *E. coli* PurR is a two-domain protein having an NH_2-terminal DNA binding domain joined to a domain for corepressor binding and dimerization (5, 27). Hypoxanthine and guanine are the signals that reflect the availability of purine nucleotides and that function as corepressors to increase the binding affinity of PurR for a 16-bp palindromic control site (16, 23). Binding results from interactions of amino acid side chains in a "hinge helix" and a helix-turn-helix motif from each subunit in the minor groove and symmetry-related major grooves, respectively, of the DNA control site (27).

B. subtilis PurR, on the other hand, resembles a two-domain protein with an NH_2-terminal DNA binding domain joined to a phosphoribosyltransferase-like effector binding domain (31), although this structure-function model has not been verified experimentally. PurR residues 72 to 276 have sequence similarity to *B. subtilis* xanthine phosphoribosyltransferase (25% identity), but phosphoribosyltransferase activity with xanthine, guanine, or adenine was not detected (data not shown). This finding contrasts with the characteristics of the *B. subtilis* pyrimidine repressor, which is a uracil phosphoribosyltransferase (29). Purified *B. subtilis* PurR binds to an extended region of the *pur* operon, as reported previously for the crude repressor (11, 31). The present data also establish that the purified repressor binds to *purA*, *purR*, and *pyr* operon 5′-flanking DNA. The recognition sequence for this binding has not been determined, although a GAAC-N_{24}-GTTC sequence in the *pur* operon was shown by methylation interference and mutagenesis to function in binding. A role for this sequence in *pur* operon regulation has not been investigated. A GAAT-N_{25}-GTTC symmetry is also found in a similar position in the *purA* control region (18), and closely related sequences are present in *purR* and in the *pyr* operon. Given the very similar PurR binding affinity and footprints for the *pur* operon and *purA*

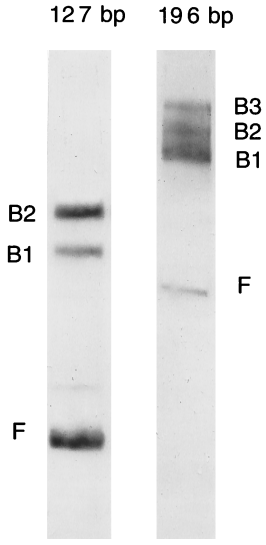

FIG. 7. PurR-*pur* operon binding stoichiometry. An autoradiograph is shown for a PurR-DNA gel shift assay with ^{35}S-labeled PurR and ^{32}P-labeled *pur* operon fragments from −147 to −21 and from −193 to +3. Free (F) and bound (B1, B2, and B3) species are indicated.

TABLE 2. Molar ratios for PurR dimer-DNA binding

Complex	PurR dimer-DNA ratio detected with the following fragment:	
	127 bp	196 bp
B3	ND[a]	5.57 ± 0.66
B2	2.00 ± 0.27	2.30 ± 0.20
B1	2.27 ± 0.32	1.78 ± 0.10
F	0	0

[a] ND, not detected.

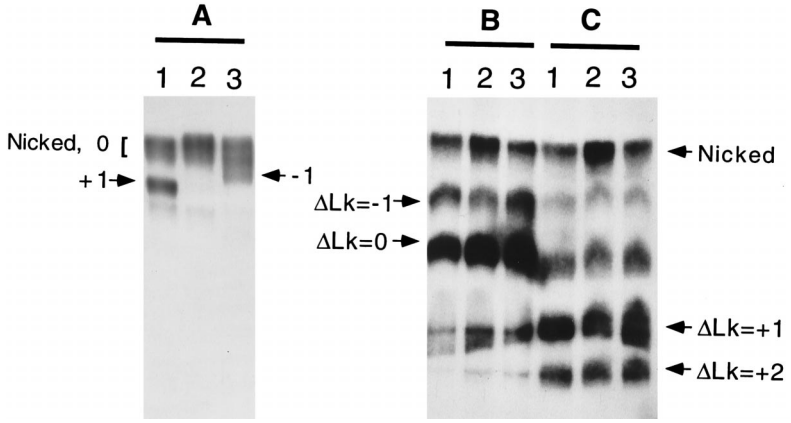

FIG. 8. Minicircle topoisomers and the torsional constraint assay. (A) Analysis of topoisomers arising from self-ligation of a 628-bp DNA fragment containing the *pur* operon control site on a 4% polyacrylamide gel (not containing ethidium bromide). Self-ligation was performed in the presence of 0 (lane 1), 0.15 (lane 2), or 0.30 (lane 3) μg of ethidium bromide per ml, yielding three samples (labeled 1, 2, and 3) with different degrees of supercoiling. With electrophoresis in the absence of ethidium bromide, the degree of supercoiling of the closed minicircles ranged from +1 to −1 in samples 1 to 3, respectively. The positions of these topoisomers and the nicked circles are indicated. (B and C) Portions of DNA samples 1 to 3 from panel A were incubated with topoisomerase I in the absence of PurR (B) or after preincubation with PurR (C). The resultant purified DNA was analyzed on a 4% polyacrylamide gel containing 0.3 μg of ethidium bromide per ml so that all of the topoisomers were positively supercoiled. The relaxed unconstrained minicircles, the predominant topoisomer form in panel B, lanes 1 to 3, are designated ΔLk = 0 and served as the reference state. ΔLk values for the other topoisomers, based upon their mobilities with respect to the reference state, are indicated.

control sites, a common recognition element is expected. However, mutational analysis of the GAAC-N_{25}-GTTC motif in *purA* failed to support an essential role in PurR binding (data not shown). Thus, no evidence that identifies a common PurR DNA recognition element is available.

The four PurR binding sites having essentially no sequence similarity other than the motif noted above resemble OxyR control sites. OxyR is a transcriptional regulator of the LysR family that activates the expression of defense genes in response to oxidative stress in *E. coli* (28). OxyR footprints span 45 bp, and six previously characterized sites have only three conserved base pairs. A consensus binding motif of ATAG-N_7-CTAT-N_7-ATAG-N_7-CTAG was identified by selection of random synthetic sequences. However, key nucleotides in both the natural and the synthetic sites diverge from the consensus motif. The ATAG dyad in synthetic OxyR sites conforms to the more limited T-N_{11}-A binding motif for LysR transcriptional regulators (14). It was proposed that OxyR achieves tight specific binding by the combination of four contacts of intermediate affinity, rather than by the more common interaction of symmetry-related helix-turn-helix DNA binding motifs with a single palindromic site. In this context, unidentified *pur* operon sites flanking the GAAC-N_{24}-GTTC motif may be required to support high-affinity binding of PurR. In preliminary experiments, deletions from the 5′ or 3′ ends of the −147 to −21 *pur* operon control site decreased binding affinity (32). However, it was not determined if reduced PurR binding affinity was due to deletion of specific flanking sites or to a decreased overall DNA fragment length.

High-affinity PurR binding to DNA takes place in the absence of an effector molecule and likely involves wrapping of DNA around the repressor. A linking number change of +1 for control site DNA minicircles bound to PurR suggests that one positive superhelical turn is wrapped around PurR, perhaps similar to the wrapping of approximately one turn of DNA around DNA gyrase (20). An A/T sequence periodicity at approximately 10-bp intervals in the *pur* operon between nts −115 and −50 was noted previously (11) and is similar to that observed for DNA bound by histone octamers (25) and DNA gyrase (30). One possibility is that PurR binds to a *pur* operon DNA control site having a GAAC-N_{24}-GTTC core sequence that can wrap around the protein. Based on the PurR-DNA stoichiometry, the protein core would appear to contain two molecules of PurR dimer. Given the proximity of the PurR binding site to the −35 promoter element, this protein-DNA interaction should block the access of RNA polymerase to the promoter, thus inhibiting transcription initiation.

There is evidence that the interaction of PurR with its 5′-flanking control site represses transcription initiation of the *pur* operon (10, 11, 31) and represses the expression of *purR* (31). PurR was also recently shown to regulate the expression of *purA* in *B. subtilis* (21). Although we observed specific binding of PurR to the *pyr* operon promoter region, initial experiments have not detected the regulation of *pyr* operon expression by *purR* (7). It should be noted that the *E. coli* purine repressor binds to two *pyr* genes and provides purine-mediated regulation (4, 34) in addition to the expected, stronger pyrimidine-specific control. This coregulation may contribute to balancing purine and pyrimide nucleotide pools.

PRPP is the effector that modulates PurR binding to DNA, acting as an inducer to inhibit the binding of a repressor protein to a control site. According to the hypothesis for PurR binding, PRPP may act to interfere with either the recognition of a DNA sequence or DNA wrapping. Whatever the exact details for the protein-DNA interaction, PurR represses transcription initiation by a unique mechanism not yet seen for other transcriptional regulators.

ACKNOWLEDGMENTS

This work was supported by U.S. Public Health Service grants GM24658 (to H.Z.) and GM48341 (to A.S.).

REFERENCES

1. **Arnvig, K., B. Hove-Jensen, and R. L. Switzer.** 1990. Purification and properties of phosphoribosyl-diphosphate synthetase from *Bacillus subtilis*. Eur. J. Biochem. **192:**195–200.
2. **Ausubel, F. M., R. Brent, R. E. Kingston, D. D. Moore, J. G. Seidman, J. A. Smith, and K. Struhl.** 1989. Current protocols in molecular biology. Green Publishing Associates and Wiley Interscience, New York, N.Y.
3. **Budisa, N., B. Steipe, P. Demanzl, C. Eckerskorn, J. Kellermann, and R. Huber.** 1995. High-level biosynthetic substitution of methionine in proteins by its analogs 2-aminohexanoic acid, selenomethionine, telluromethione and ethionine in *Escherichia coli*. Eur. J. Biochem. **230:**788–796.
4. **Choi, K. Y., and H. Zalkin.** 1990. Regulation of *Escherichia coli pyrC* by the

purine regulon repressor protein. J. Bacteriol. **172:**3201–3207.
5. **Choi, K. Y., and H. Zalkin.** 1992. Structural characterization and corepressor binding of the *Escherichia coli* purine repressor. J. Bacteriol. **174:**6207–6214.
6. **Crick, F. H. C.** 1976. Linking numbers and nucleosomes. Proc. Natl. Acad. Sci. USA **73:**2639–2643.
7. **D'Elia, J., and R. L. Switzer.** Unpublished data.
8. **Depew, R. E., and J. C. Wang.** 1975. Conformational fluctuations of DNA helix. Proc. Natl. Acad. Sci. USA **72:**4275–4279.
9. **Doherty, A. J., S. R. Ashford, J. A. Brannigan, and D. B. Wigley.** 1995. A superior host strain for the overexpression of cloned genes using the T7 promoter based vectors. Nucleic Acids Res. **23:**2074–2075.
10. **Ebbole, D. J., and H. Zalkin.** 1987. Cloning and characterization of a 12-gene cluster from *Bacillus subtilis* encoding nine enzymes for *de novo* purine nucleotide synthesis. J. Biol. Chem. **262:**8274–8287.
11. **Ebbole, D. J., and H. Zalkin.** 1989. Interaction of a putative repressor protein with an extended control region of the *Bacillus subtilis pur* operon. J. Biol. Chem. **264:**3553–3561.
12. **Fuller, F. B.** 1971. The writhing number of a space curve. Proc. Natl. Acad. Sci. USA **68:**815–819.
13. **Germond, J. E., B. Hirt, P. Oudet, M. Gross-Bellard, and P. Chambon.** 1975. Folding of the DNA double helix in chromatin-like structures from simian virus 40. Proc. Natl. Acad. Sci. USA **72:**1843–1847.
14. **Goethals, K., M. V. Montagu, and M. Holsters.** 1992. Conserved motifs in a divergent *nod* box of *Azorhizobium caulinodans* ORS571 reveal a common structure in promoters regulated by LysR-type proteins. Proc. Natl. Acad. Sci. USA **89:**1646–1650.
15. **Goulet, I., Y. Zivanovic, and A. Prunell.** 1988. Chromatin reconstitution on small DNA rings. J. Mol. Biol. **200:**253–266.
16. **Houlberg, U., and K. F. Jensen.** 1983. Role of hypoxanthine and guanine in regulation of *Salmonella typhimurium pur* gene expression. J. Bacteriol. **153:** 837–845.
17. **Krämer, H., M. Amouyal, A. Nordheim, and B. Müller-Hill.** 1988. DNA supercoiling changes the spacing requirement of two *lac* operators for DNA loop formation with *lac* repressor. EMBO J. **7:**547–556.
18. **Mäntsälä, P., and H. Zalkin.** 1992. Cloning and sequence of *Bacillus subtilis purA* and *guaA*, involved in the conversion of IMP to AMP and GMP. J. Bacteriol. **174:**1883–1890.
19. **Ogasawara, N., S. Nakai, and H. Yoshikawa.** 1994. Systematic sequencing of the 180 kilobase region of the *Bacillus subtilis* chromosome containing the replication origin. DNA Res. **1:**1–14.
20. **Orphanides, G., and A. Maxwell.** 1994. Evidence for a conformational change in the DNA gyrase-DNA complex from hydroxy radical footprinting. Nucleic Acids Res. **22:**1567–1575.
21. **Rappu, P., Zalkin, H., and P. Mäntsälä.** Unpublished data.
22. **Rhodes, D., and A. Klug.** 1980. Helical periodicity of DNA determined by enzyme digestion. Nature **286:**573–578.
23. **Rolfes, R. J., and H. Zalkin.** 1990. Purification of the *Escherichia coli* purine regulon repressor and identification of corepressors. J. Bacteriol. **172:**5637–5642.
24. **Sambrook, J., E. F. Fritsch, and T. Maniatis.** 1989. Molecular cloning: a laboratory manual, 2nd ed. Cold Spring Harbor Laboratory, Cold Spring Harbor, N.Y.
25. **Satchwell, S. C., H. R. Drew, and A. A. Travers.** 1986. Sequence periodicities in chicken nucleosome core DNA. J. Mol. Biol. **191:**659–675.
26. **Saxild, H. H., and P. Nygaard.** 1991. Regulation of levels of purine biosynthetic enzymes in *Bacillus subtilis*: effects of changing purine nucleotide pools. J. Gen. Microbiol. **137:**2387–2394.
27. **Schumacher, M. A., K. Y. Choi, H. Zalkin, and R. G. Brennan.** 1994. Crystal structure of lacI member, PurR, bound to DNA: minor groove binding by α helices. Science **266:**763–770.
28. **Toledano, M. B., I. Kullik, F. Trinh, P. T. Baird, T. C. Schneider, and G. Storz.** 1994. Redox-dependent shift of OxyR-DNA contacts along an extended DNA-binding site: a mechanism for differential promoter selection. Cell **78:**897–909.
29. **Turner, R. J., Y. Lu, and R. L. Switzer.** 1994. Regulation of the *Bacillus subtilis* pyrimidine biosynthetic (*pyr*) gene cluster by an autogenous transcriptional attenuation mechanism. J. Bacteriol. **176:**3708–3722.
30. **Wahle, E., and A. Kornberg.** 1988. The partition locus of plasmid pSC101 is a specific binding site for DNA gyrase. EMBO J. **7:**1889–1895.
31. **Weng, M., P. L. Nagy, and H. Zalkin.** 1995. Identification of the *Bacillus subtilis pur* operon repressor. Proc. Natl. Acad. Sci. USA **92:**7455–7459.
32. **Weng, M., and H. Zalkin.** Unpublished data.
33. **White, J. H.** 1969. Self-linking and the Gauss integral in higher dimensions. Am. J. Math. **91:**693–728.
34. **Wilson, H., and C. L. Turnbough, Jr.** 1990. Role of the purine repressor in the regulation of pyrimidine gene expression in *Escherichia coli* K-12. J. Bacteriol. **172:**3208–3213.
35. **Zivanovic, Y., I. Goulet, and A. Prunell.** 1986. Properties of supercoiled DNA in gel electrophoresis: the U-like dependence of mobility on topological constraint. DNA-matrix interactions. J. Mol. Biol. **192:**645–660.